AC

US–FT/15–94

Scaling behaviour and correlations in the String Fusion Model for heavy ion collisions

su8444

N. Armesto, M. A. Braun[1], E. G. Ferreiro and C. Pajares
Departamento de Física de Partículas,
Universidade de Santiago de Compostela,
15706–Santiago de Compostela, Spain

Abstract

The KNO scaling, the scaling of multiplicities, the behaviour of fluctuations in the transverse momentum as a function of the multiplicity and the long range correlations in nucleus–nucleus collisions are studied by a Monte Carlo code based on the String Fusion Model. It is shown that the fusion of strings produces a strong reduction of the long range correlations at high multiplicities, which could be detected experimentally. On the contrary the KNO scaling, the scaling of multiplicities and the behaviour of fluctuations in the transverse momentum are not modified when string fusion is included.

US–FT/15–94
October 1994

[1] On leave of absence from the Department of High Energy Physics, University of St. Petersburg, 198904 St. Petersburg, Russia.

1 Introduction

In the last years much effort has been done in the search of the Quark Gluon Plasma (QGP). This problem appears to be complicated so that more theoretical and experimental material is needed to obtain the wished goal ([1]). One of the main points in this search is to know how the QGP can be reached in the framework of the usual models of hadronic interactions ([2, 3, 4, 5, 6]). In these models strings or Pomerons are exchanged between the projectile and target. The number of strings grows with the energy and with the number of nucleons of the participant nuclei. In the first approximation strings fragment into particles or resonances in an independent way. However, the interaction between strings may become important with their number growing. This interaction has been introduced into some of the models ([7, 8, 9, 10, 11]). In particular, the fusion of strings has been incorporated into the Dual Parton Model (DPM) and the Quark Gluon String Model (QGSM). It may be regarded as an intermediate stage between nucleon–nucleon collisions and the QGP.

On the other hand, models based on independent nucleon–nucleon interactions satisfy several scaling laws, like Koba–Nielsen–Olesen (KNO) scaling ([12]) or scaling of multiplicities ([13, 14]), and give definite predictions for the short and long range correlations. In this paper these observables are studied at Super Proton Syncrotron (SPS), Relativistic Heavy Ion Collider ($RHIC$) and Large Hadron Collider (LHC) energies, using a Monte Carlo code based on the QGSM, both without interaction of strings and with their fusion. The aim of this paper is not to give detailed predictions of the model but to select observables which are sensitive to collective effects such as the interactions between strings.

The paper is organized as follows: In the next two Sections the String Fusion Model and the Monte Carlo code based on it are briefly described. In Section 4 the results of our Monte Carlo code on the KNO scaling for nucleus–nucleus collisions with and without string fusion are compared. In Section 5 the fluctuations in the transverse momentum distribution as a function of the charged multiplicity for pp, $p\alpha$, $\alpha\alpha$ and SPb collisions are computed and compared with the existing experimental data. In Section 6 the scaling of multiplicities is checked. In Section 7 the modifications of the long range correlations due to string fusion are discussed and, finally, in Section 8 our conclusions are presented.

2 The String Fusion Model

It is possible to imagine different physical scenarios for the interaction of strings. In the simplest one several strings merge into one of the same type, quite similarly to the multipomeron interaction in the Regge–Gribov theory. A richer and more general picture follows if one assumes the existence of various types of strings with different colour contents. When two strings are close in transverse space they may form a new string, which corresponds to a double colour exchange in the Abelian case ([8]). More generally one can assume that any number of strings characterized by their "colour numbers" $n_1, n_2, ...$ fuse into one with colour number $n = \sum n_i$ when their transverse space positions are close. The usual string corresponds to $n = 1$.

Let the number of strings with colour number n be ν_n. The total number of strings is $M = \sum \nu_n$, $n = 1, 2, ...$ and the total colour number is $N = \sum n\nu_n$. If two strings, each one with a transverse area a_0, fuse into a new one, the probability for them to exist separately in the total transverse area a will be disminished by a factor $1 - x$, where $x = a_0/a$ is the probability of fusion. With three strings the inhibition factor becomes $(1 - x)(1 - 2x)$ and so on, until we come to the point when $1 - N_{max} \leq 0$ and no more strings can coexist in the area a. In this manner we arrive ([8]) at the probability distribution $p(\nu_n)$ for having ν_n strings of type n,

$$p(\nu_n) = c(Q^N/[\prod \nu_n! \prod (n!)^{\nu_n}])x^{N-M} \prod_{k=1}^{M-1} (1 - kx) \quad , \tag{1}$$

where parameter Q has a meaning of the average colour.

The normalization of $p(\nu_n)$ fixes c as

$$c^{-1} = \{1 + g\}^{1/x} \quad , \tag{2}$$

where

$$g = \sum_{n=1} (Qx)^n/n! = \exp(Qx) - 1 \tag{3}$$

and $\{...\}^\alpha$ denotes the truncated binomial series with positive binomial coefficients.

Assuming that for a given number of strings ν_n of type n the scattering matrix is a product of individual matrices s_n for all strings, the total S–matrix is given by the product

$$S(b) = \sum_{\nu_n} p(\nu_n) \prod s_n^{\nu_n}(b) \quad , \tag{4}$$

which results in

$$S(b) = \{1 + s^{(r)}(b)\}^{1/x}/\{1 + g\}^{1/x} \quad , \tag{5}$$

where the "renormalized" elementary S–matrix is given by

$$s^{(r)}(b) = \sum_{n=1} (Qx)^n s_n(b)/n! \quad , \tag{6}$$

which effectively takes into account contributions of all colours. The S–matrix given in Eq. (5) is unitary by construction, provided the elementary S–matrix is unitary.

Starting from Eq. (5) one can separate the amplitude first into contributions from a given number M of exchanged strings of any type, and then, following the AGK cutting rules ([15]), into contributions from k cut and $M-k$ uncut strings. Fixing k and summing over all possible numbers of uncut strings one arrives at the cross section σ_k with k cut strings of any type:

$$\begin{aligned} \sigma_k(b) &= (\sigma(b))^k C^k_{1/x}(1+g-\sigma(b))^{1/x-k}/\{1+g\}^{1/x} \quad , \\ \sigma(b) &= 2Im\ a^{(r)}(b) \quad . \end{aligned} \tag{7}$$

If we sum $k\sigma_k$, then, according to the AGK rules, we obtain what may be interpreted as an effective single Pomeron exchange σ_P:

$$\sigma_P(b) = \sigma(b)/(x(1+g)) \quad . \tag{8}$$

Denoting $\sigma(0) = \xi g$, we find that ξ is bounded by unitarity. Then $\sigma_P(0)$ can grow with $s = E^2_{cm}$ only as $1/x$, that is, as $\ln s$, and never as s^Δ as for a supercritical Pomeron. In this sense the interaction introduced in Eq. (1) transforms the Pomeron from a supercritical one into a nearly critical one. However, at realistic energies, g is small, so that $\sigma_P(0)$ may mainly grow because of the growth of g which may be exponential.

A more detailed cross section for $k_1, k_2, ...$ cut strings of colour numbers $1, 2, ...$, $\sigma_{k_1 k_2 ...}$, is given by

$$\sigma_{k_1 k_2 ...}(b) = (k!/\prod k_n!) \prod_n (\sigma^{(r)}_n(b))^{k_n} C^k_{1/x}(1+g-\sigma(b))^{1/x-k}/\{1+g\}^{1/x} \quad , \tag{9}$$

where $k = \sum k_n$. To integrate over b we assume that all $\sigma^{(r)}_n(b)$ are gaussians with the same R^2. Then

$$\sigma_{k_1 k_2 ...} = (k!/\prod k_n!) \prod_n z_n^{k_n} \sigma_k \quad , \tag{10}$$

where

$$z_n = \frac{\sigma^{(r)}_n(0)}{\sigma(0)} \quad , \quad 0 \le z_n \le 1 \quad , \quad \sum z_n = 1 \quad . \tag{11}$$

The multiplicity μ is given in terms of the multiplicity μ_n of the string of colour n,

$$\mu = \sum_{k_1, k_2, ...} \sigma_{k_1 k_2 ...} \sum_n k_n \mu_n / \sigma^{in} \quad . \tag{12}$$

From Eqs. (10) and (12) one obtains

$$\mu =< k > \sum_n z_n \mu_n \quad , \tag{13}$$

where the mean number of cut strings $< k >$ is

$$< k >= \sum_k k\sigma_k/\sigma^{in} = \pi R^2 \sigma_P(0)/\sigma^{in} = \pi R^2 \sigma(0)/[x(1+g)\sigma^{in}] \quad . \tag{14}$$

In the same way the average $< p_\perp^2 >_N$ can be studied. Assuming that for the string of colour n $< p_\perp^2 >_n = \chi^2 n^\alpha$,

$$< p_\perp^2 >= \chi^2 \sum_n z_n n^\alpha \quad . \tag{15}$$

Formulae for μ and $< p_\perp^2 >$ essentially depend on the parameters z_n describing the relative strength of the interactions with different types of strings. We do not know these values a priori and we will do some simple assumptions. The simplest one is that $\sigma_n(0)$ factorizes in the spirit of the eikonal models,

$$\sigma_n(0) = \sigma_1^n(0) \quad , \tag{16}$$

where σ_1 is determined from the condition $\sum z_n = 1$. Then

$$z_n = u^n/(g\xi n!) \quad , \quad u = \ln(1+g\xi) \quad , \tag{17}$$

which, assuming $\mu_n = n\mu_1$ and $\alpha = 1$, gives rise to

$$\mu = \mu_1 < k > f(u) \quad , \quad < p_\perp^2 >= \chi^2 f(u) \quad , \tag{18}$$

$$f(u) = ue^u/(e^u - 1) \quad . \tag{19}$$

A different assumption like

$$\sigma_n(0)/n! = \sigma_1^n(0) \tag{20}$$

leads to a faster growth of μ and $< p_\perp^2 >$ with energy. In this case

$$z_n = u^n/(g\xi) \quad , \quad u = g\xi/(1+g\xi) \tag{21}$$

and Eq. (18) stands for μ and $< p_\perp^2 >$ but now

$$f(u) = 1 + g\xi \quad . \tag{22}$$

In order to compute the average transverse momentum at fixed multiplicity we evaluate $< p_\perp^2 >_N$ for fixed $N = \sum n k_n$. Other observables, like $(Dp_\perp^2)_N$ or $< p_\perp >_N$, can be treated in an analogous way. Presenting $\delta_{N,\sum nk_n} = \oint (dy/2\pi i y) y^{-N+\sum nk_n}$ we obtain for the cross section σ_N at a given N

$$\sigma_N = \sum_k \sigma_k \oint \frac{dy}{2\pi i y} y^{-N} (\sum \rho_n)^k \quad , \tag{23}$$

with $\rho_n = z_n y^n$.

In the first case (Eq. (20)) this formula gives

$$\sigma_N = \sum_k \sigma_k (1/(g\xi))^k C_{N-1}^{k-1} u^N \quad . \tag{24}$$

In the second case (Eq. (16)) we obtain

$$\sigma_N = \frac{u^N}{N!} \sum_k \sigma_k S_{k,N} (-1/(g\xi))^k \quad , \tag{25}$$

where

$$S_{k,N} = \sum_{l=0}^{k} C_l^k l^N (-1)^l \quad , \qquad S_{k,N} = 0 \quad \text{if} \quad N < k \quad . \tag{26}$$

To compute $< p_\perp^2 >_N$ we have to evaluate

$$I = \oint \frac{dy}{2\pi i y} y^{-N} \rho_n (\sum \rho_n)^{k-1} \quad . \tag{27}$$

In the first case it turns out to be

$$I = (1/(g\xi))^k u^N C_{N-n-1}^{k-2} \text{ with the requirement that } C_{-1}^{-1} \equiv 1 \quad , \tag{28}$$

so that

$$\sigma_N < p_\perp^2 >_N = \sum_{n,k} (1/(g\xi))^k u^N C_{N-n-1}^{k-2} \sigma_k < p_\perp^2 >_n \quad . \tag{29}$$

In the second case

$$I = (1/(g\xi))^k u^n T_{k-1,N-n}/n! = (-1)^{k-1} S_{N-n,k-1} u^N / [(g\xi)^k n! (N-n)!] \tag{30}$$

and therefore

$$\sigma_N < p_\perp^2 >_N = u^N \sum_{n,k} \sigma_k < p_\perp^2 >_n (-1)^{k-1} S_{N-n,k-1} / [(g\xi)^k n! (N-n)!] \quad . \tag{31}$$

The string fusion model has been applied to the study of hA and AB interactions ([9]). For hA interactions, repeating the arguments that led to Eqs. (1) and (5), the probability for the interacion of the projectile with l target nucleons is

$$p^{(l)}(\nu_n^{(1)}, \nu_n^{(2)}, ...) = c_l (Q^N / [\prod_{i,n} \nu_n^{(i)}! (n!)^{\nu_n^{(i)}}]) x^{N-M} \prod_{k=1}^{M-1} (1 - kx) \quad , \tag{32}$$

where $\nu_n^{(i)}$ is the number of strings of type n produced in the interaction of the projectile with the i–th target nucleon from l active ones. Now $N = \sum_{i,n} n\nu_n^{(i)}$ and $M = \sum_{i,n} \nu_n^{(i)}$ are respectively the total colour and the number of strings produced by all the l interacting nucleons. The S–matrix for a process with fixed l and transverse nucleon positions $b_1, ..., b_l$ will be given by

$$S^{(A)}_{l,b_1,...,b_l} = \prod_{i=1}^{l} (\sum_{\nu_n^{(i)}} s_n^{\nu_n^{(i)}}(b_i)) p^{(l)}(\nu_n^{(i)}) \quad , \tag{33}$$

which turns out to be

$$S^{(A)}_{l,b_1,...,b_l} = \{1 + s_l^{(r)}(b_1, ..., b_l)\}^{1/x} / \{1 + lg\}^{1/x} \quad , \tag{34}$$

where

$$s_l^{(r)}(b_1, ..., b_l) = \sum_{i=1}^{l} s^{(r)}(b_i) \quad . \tag{35}$$

g is given by Eq. (3) and $s^{(r)}(b)$ by Eq. (6). $s_n(b)$ is the same S–matrix for the string of type n which appears in hh interactions.

The total hA scattering matrix $S^{(A)}(b)$ is given by

$$S^{(A)}(b) = \sum_{l=0}^{A} S_l^{(A)}(b) \quad , \tag{36}$$

where

$$S_l^{(A)}(b) = C_A^l T_A^l(b)(1 - s_0 T_A(b))^{A-l} \int_{a_0} \prod_{i=1}^{l} d^2 b_i S^{(A)}_{l,b_1,...,b_l} \quad , \tag{37}$$

$a_0 = \pi R_0^2 \simeq \sigma^{in}$ being the transverse size of each nucleon and $T_A(b)$ the profile function of the nucleus A.

From Eqs. (36) and (37) the single and double differential multiplicities $\mu^{(A)}(q)$ and $\mu^{(A)}(q_1, q_2)$ are deduced. These are generally related to the corresponding multiplicities for hN collisions by the relations

$$\mu^{(A)}(q) = \alpha \mu^{(1)}(q) \quad , \tag{38}$$

$$\mu^{(A)}(q_1, q_2) = \alpha \mu^{(1)}(q_1, q_2) + \beta \mu^{(A)}(q_1) \mu^{(A)}(q_2) \quad . \tag{39}$$

With no interaction between strings, the standard values for α and β are

$$\alpha = \nu_A = A\sigma^{(1)} / \sigma_{in}^{(A)} \quad , \qquad \beta = \lambda_A = \sigma_{in}^{(A)} w_2 \quad , \tag{40}$$

where $w_2 = \int d^2 b T_A^2(b)$. Evidently α rises as $A^{1/3}$ and β is independent of A and very close to 1 for typical nuclear distributions.

The interaction of strings changes α and β. In the limiting case of strong fusion $g \gg 1$ with a large number of exchanged strings $x \ll 1$,

$$\alpha = 1 \quad \text{and} \quad \beta \simeq 1 - \sigma^{(1)}/2\pi r^2 \quad , \tag{41}$$

where r is the radius of the Pomeron.

The generalization to AB collisions is straightforward although the geometry of the process naturally becomes much more complicated. For this reason it is natural to resort to Monte Carlo simulations, in which geometrical problems present no difficulty.

3 Monte Carlo String Fusion Model

Based on the fusion of strings, two different Monte Carlo codes ([16, 17]) have been built up taking as the underlying dynamics the DPM (or QGSM, a small variation of it). Both of them have been applied to describe most of the existing experimental data on hadron–hadron, hadron–nucleus and nucleus–nucleus collisions. In this paper the code presented in Ref. [16] is used. A hadron or nucleus collision is assumed to be an interaction between clouds of partons formed long before the collision. The distribution in the number of partons, which is directly connected with the values of the different Pomeron vertices ([18]), takes the poissonian form

$$P(n) = \gamma^n \exp(-\gamma)/n! \quad , \tag{42}$$

with the mean number of partons γ growing with energy,

$$\gamma = \gamma_0^{\Delta} \quad , \quad \Delta = 0.09 \quad , \quad \gamma_0 = g/\sigma_P^{0.5} \quad , \quad g = 1.8 \ \ GeV^{-1} \quad . \tag{43}$$

σ_P is the parton–parton cross section which is assumed to be constant, $\sigma_P = 3.5\ mb$. The parton distribution in impact parameter, relative to the center of the hadron to which they belong, is taken to be gaussian. Accordingly, a gaussian form is also taken for the $p_\perp$ distribution. Our partons are either valence quarks or diquarks or quark–antiquark pairs from the sea, with a longitudinal momentum distribution corresponding to the QGSM (which is given by Regge theory).

Without string fusion partons are assumed to interact only once. Each parton–parton interaction leads to the creation of colour strings. Since both the projectile and target should remain colourless, colour strings have to be formed in pairs. Only u, d and s quarks are considered. The s-quark suppression factor was taken $\lambda_s = 0.29$.

Hadrons and nuclei are considered on the same footing. The nuclear wave function is taken as a convolution of the parton distribution within a nucleus and the distribution of nucleons in the nucleus given by the Woods–Saxon formula. At energies larger than $\sqrt{s} = 40\ GeV$, semihard and hard collisions can be considered by means of the PYTHIA code ([19]).

We assume that strings fuse when their transverse positions come within a certain interaction area. The fusion can take place only when the rapidity intervals of the strings overlap, and allows partons to interact several times, the number of interactions being the same for projectile and target. The quantum numbers of the fused string are given by the interacting partons and its energy–momentum is evidently the sum of the energy–momenta of the ancestor strings. The colour charges at the fusing string ends sum into the colour charge of the resulting string according to the $SU(3)$ composition laws. In particular two triplet strings fuse into a antitriplet and a sextet string being 1/3 and 2/3 their respective relative probabilities. A triplet and an antitriplet string give rise to a singlet and an octet string with probabilities 1/9 and 8/9. In the present calculations fusion of only two strings was considered.

The breaking of a fused string is due to the production of two (anti)quark complexes with the same colour charges Q and $\overline{Q}$ as those at the ends of the string. The probability rate is given by the Schwinger formula ([20, 21, 22])

$$w \sim K_{[N]}^2 \exp\left(-\pi M_t^2 / K_{[N]}\right) \quad , \tag{44}$$

where $K_{[N]}$ is the tension of the string with (anti)quark complexes in the $[N]$ $SU(3)$ representation. $K_{[N]}$ is proportional to the quadratic Casimir operator C^2 for the corresponding representation:

$$C_{[3]}^2 = 4/3 \quad , \quad C_{[6]}^2 = 10/3 \quad , \quad C_{[8]}^2 = 3 \quad . \tag{45}$$

Therefore the [8] and [6] fused strings have a larger string tension which gives rise to a larger heavy flavor content. Further details and a comparison to experimental data can be found in Refs. [16] and [19].

4 Koba–Nielsen–Olesen (KNO) scaling

Long before the experiments on nucleus–nucleus collisions were done, it had been predicted that in a wide energy range around $\sqrt{s} = 20\ GeV$ the Wroblewski law and

the KNO scaling would be approximately satisfied ([23]). The experiments confirmed these predictions. In this section we would like to answer two questions: Is KNO scaling independent of string fusion? and Is KNO scaling valid at higher energies (as $RHIC$ energy)?

It is expected that the effects of string fusion are noticeable only at high multiplicities and no effect will be seen at low multiplicities. Since $\psi(z) =< n > \sigma_n/\sigma$, as a function of $z = n/ < n >$ (n is the number of charged particles) is normalized to unity, it cannot be changed only at high multiplicities, but has to be changed at low multiplicities as well. As a consecuence, we do not expect large variations in the KNO scaling function due to string fusion. This is confirmed by the results of our Monte Carlo simulations as shown in Figs. 1, 2 and 3, where the KNO scaling function is plotted both without and with fusion for $PbPb$ collisions at $\sqrt{s_{NN}} = 19.4\ GeV$ and SS and $CuCu$ collisions at $\sqrt{s_{NN}} = 200\ GeV$ respectively. To compare the tails of the distributions, in Fig. 4 the multiplicity distribution for $CuCu$ collisions at $\sqrt{s_{NN}} = 200$ GeV is also plotted. We stress that in our code no cascading of secondaries is included. This mechanism will shift to the right the high multiplicity tail of the distribution in both cases, without and with fusion. This effect would not appear in the KNO function. The comparison of Figs. 1, 2 and 3 shows a slightly different behaviour for the different projectile and target nuclei.

5 Fluctuations in transverse momentum distributions

It was pointed out long ago ([24, 25]) that the study of fluctuations of the average transverse momentum in each event, normalized to the average transverse momentum, at a given multiplicity, as a function of the inverse multiplicity, could shed light on the study of multiparticle dynamics, concretely on the fluctuations of the temperature of the source, once the statistical contribution to such fluctuations is separated. Unfortunately, except for the pp, $p\alpha$ and $\alpha\alpha$ ISR results, there are no hadron–hadron or nucleus–nucleus data published up to now. Only the NA36 Collaboration at SPS is analyzing their data in this sense.

On the statistical basis, the behaviour of $(Dp_\perp/ < p_\perp >)^2$ as a function of $1/n$ (n is the number of charged particles) should be a straight line, going to zero as n goes to

infinity. A departure from this behaviour has a dynamical origin.

In Figs. 5, 6, and 7 the results of our Monte Carlo code without and with fusion of strings are plotted for pp collisions at $\sqrt{s} = 63\ GeV$, for $p\alpha$ at $\sqrt{s_{NN}} = 44\ GeV$ and for $\alpha\alpha$ at $\sqrt{s_{NN}} = 31.2\ GeV$, together with the experimental data. Fusion seems to produce no effect. The experimental data are somewhat higher than the theoretical ones, especially at low multiplicities and for pp collisions. We do not know exactly what is the origin of this excess in the transverse momentum distribution. One possibility is the contribution of semihard and hard interactions, not included in our code. This might explain that the discrepancy is larger at higher energies. Unfortunately, there is no data on heavier nucleus collisions.

In Fig. 8 our results for SPb collisions at $\sqrt{s_{NN}} = 200\ GeV$ are presented. There seems to be a trace of a departure of the straight line behaviour with string fusion, for which the curve goes up a bit steeper.

6 Scaling of multiplicities

The scaling of multiplicities means that the ratio of particle densities $\rho_n(y = 0)\ /\ <\rho(y=0)>$ is equal to the ratio of charged secondaries $z = n/ < n >$. It was noted in Refs. [13] and [14] that any deviation from it in nucleus–nucleus collisions could point out the existence of collective effects. In Figs. 9 and 10 the results of our Monte Carlo calculations are presented for $PbPb$ collisions at $\sqrt{s_{NN}} = 6300\ GeV$ and for $CuCu$ collisions at $\sqrt{s_{NN}} = 200\ GeV$ respectively. A perfect scaling is obtained both with and without fusion.

7 Long range correlations

Recently it has been proposed ([26]) that the study of forward–backward correlations in nucleus–nucleus collisions at high energies may serve as a method to clearly detect the fusion of strings and to distinguish it from other kind of collective effects, such as the possibility of fusion of the produced hadrons into clusters.

The squared backward–forward dispersion is

$$D^2_{BF} =< n_B n_F > - < n_B >< n_F > \ , \tag{46}$$

where $n_B(n_F)$ is the number of charged particles in a backward (forward) rapidity

interval. In order to eliminate the short range correlations we consider backward and forward intervals separated by at least 1.5 rapidity units. Cluster formation ([27, 28]) implies the fusion of particles or resonances close in rapidity so the long range correlations are not affected.

In any model based on a superposition of independent exchanges (Pomerons or strings), D^2_{BF} is proportional to their mean number ([29]). With the fusion of strings, their mean number is reduced so that the long range correlations are also reduced.

For hadron–nucleus collisions, in the limit of strong fusion, the squared dispersion and the mean multiplicity (in the central region) deduced from Eqs. (38) and (39) behave like

$$D^2 \sim A^{-1/3} \quad \text{and} \quad < n > \sim const. \ , \tag{47}$$

to be compared with the behaviour without fusion $D^2 \sim A^{1/3}$ and $< n > \sim A^{1/3}$. However, these large differences can be reduced due to finite energy corrections and for more realistic fusion strength. We account for these in our Monte Carlo code. The obtained results were compared to the existing experimental data ([30, 31, 32]) on long range correlations for pp collisions at $\sqrt{s} = 45\ GeV$, for $\overline{p}p$ collisions at $\sqrt{s} = 540\ GeV$ and for pp, pAr and pXe collisions at $p_{lab} = 200\ GeV/c$. These data measure the backward multiplicity as a function of the number of forward particles, by a fit to a straight line $< n_B(n_F) >= a + bn_F$. The slope b is given by $b = D^2_{BF}/D^2_{FF}$. Our Monte Carlo results for the slope b without and with string fusion together with the experimental data are shown in Table 1. A good agreement is obtained. Unfortunately, there is no data on nucleus–nucleus collisions.

To enhance the string fusion effects we have also computed D^2_{BF} for selected events with a high charged multiplicity, larger than $n_{ch,thres}$. The squared dispersion D^2_{BF} computed in this way is shown in Fig. 11 for $PbPb$ collisions at SPS energy and in Fig. 12 for $CuCu$ collisions at $RHIC$ energy. In these two cases we generate 6000 and 10000 events respectively. At SPS energy the forward region is defined as $y_{lab} > 3.6$ and the backward one as $y_{lab} < 2.0$, while at $RHIC$ energy, the definitions are $y > 1.0$ and $y < -1.0$ respectively. In the case of $PbPb$ at SPS energy, the mean charged multiplicity reduces from 500 in the no fusion case to 470 if fusion is introduced. From Fig. 11, one observes that a sizeable difference between the no fusion and fusion case appears only for multiplicities greater than 1500, i.e. $n_{ch}/ < n_{ch} >= z > 3$, and the reduction of D^2_{BF} from the no fusion to the fusion case is about a factor 1.5. This value

of z is not yet in the tail of the distribution, see Fig. 1. Therefore it should not be difficult to obtain experimentally enough statistics to check this behaviour. In the case of $CuCu$ collisions at $\sqrt{s_{NN}} = 200\ GeV$, the mean charged multiplicity changes from 490 for the no fusion case to 440 when string fusion is introduced. In this case the effect is stronger and sizeable for multiplicities greater than 1000 ($z > 2$). For $z > 3$ the reduction from the no fusion to the fusion case is now about a factor 3. In this case, it would be quite easy to check our predictions experimentally with the Pb beam at SPS and for not so heavy nuclei at $RHIC$.

The strong suppression in the long range correlations seen in D^2_{BF} is also translated into the slope b. For $CuCu$ collisions at $\sqrt{s_{NN}} = 200\ GeV$ the reduction of b with fusion is more than a factor 2, from 0.89 to 0.39, for $z > 3.1$.

8 Conclusions

The results of the Monte Carlo code based on the QGSM show that there is no difference in the KNO scaling and in the scaling of multiplicities between the independent string model and the model with string fusion. This is also true for the dependence of the dispersion of the transverse momentum on the inverse multiplicity.

On the other hand, the long range correlations measured by the forward–backward squared dispersion are shown to be strongly reduced at high multiplicity in nucleus–nucleus collisions by the string fusion. This reduction should be detected clearly at $RHIC$ energies and could also be seen at $\sqrt{s_{NN}} = 19.4\ GeV$ for $PbPb$ collisions, although in this case the effect is smaller.

Acknowledgements

We thank A. Capella and C. Merino for useful discussions and the CICYT of Spain for financial support. We also thank J. Mosquera and M. Pló for discussions on temperature fluctuations. Also, N. A. and E. G. F. thank the Xunta de Galicia and M. A. B. the Dirección General de Política Científica of Spain for financial support.

References

[1] *Quark Gluon Plasma*, Ed. R. Hwa, World Scientific 1990.

[2] B. Andersson, G. Gustafson and B. Nilsson–Almqvist, Nucl. Phys. **B281** (1987) 289; M. Gyulassy, CERN preprint CERN–TH 4794 (1987).

[3] A. Capella, U. P. Sukhatme, C.–I. Tan and J. Tran Thanh Van, Phys. Rep. **236** (1994) 225.

[4] A. B. Kaidalov and K. A. Ter–Martirosyan, Phys. Lett. **B117** (1982) 247.

[5] K. Werner, Phys. Rep. **232** (1993) 87.

[6] H. Sorge, H. Stöcker and W. Greiner, Nucl. Phys. **A498** (1989) 567c.

[7] C. Pajares, Proceedings of the *International Workshop on Quark Gluon Plasma Signatures*, Strasbourg, France, October 1–4 1990, Ed. V. Bernard *et al.*, Editions Frontières 1991, p. 21.

[8] M. A. Braun and C. Pajares, Nucl. Phys. **B390** (1993) 542; N. Armesto, M. A. Braun and C. Pajares, Phys. Rev. **D48** (1993) 162.

[9] M. A. Braun and C. Pajares, Phys. Lett. **B287** (1992) 154; Nucl. Phys. **B390** (1993) 559; N. Armesto, M. A. Braun and C. Pajares, Santiago preprint US–FT/2–94 (1994) (submitted to Phys. Rev. **D**).

[10] B. Andersson, Proceedings of the *XXII International Symposium on Multiparticle Dynamics*, Santiago de Compostela, July 1992 , Ed. C. Pajares, World Scientific 1993, p. 428.

[11] H. Sorge, M. Berenguer, H. Stöcker and W. Greiner, Phys. Lett. **B289** (1992) 6.

[12] Z. Koba, H. B. Nielsen and P. Olesen, Nucl. Phys. **B40** (1972) 317.

[13] M. G. Ryskin and Yu. M. Shabelskiĭ, Z. Phys. **C48** (1990) 463.

[14] D. Krpic' and Yu. M. Shabelskiĭ, Z. Phys. **C48** (1990) 483; S. Backovic, D. Krpic' and Yu. M. Shabelskiĭ, Z. Phys. **C53** (1992) 613.

[15] V. A. Abramovskiĭ, V. N. Gribov and O. V. Kancheli, Yad. Fiz. **18** (1973) 595 (Sov. J. Nucl. Phys. **18** (1974) 308).

[16] N. S. Amelin, M. A. Braun and C. Pajares, Phys. Lett. **B306** (1993) 312; Z. Phys. **C63** (1994) 507.

[17] C. Merino, C. Pajares and J. Ranft, Phys. Lett. **B276** (1992) 168; H.–J. Möhring, J. Ranft, C. Merino and C. Pajares, Phys. Rev. **D47** (1993) 4142.

[18] V. A. Abramovskiĭ, E. V. Gedalin, E. G. Gurvich and O. V. Kancheli, Sov. J. Nucl. Phys. **53** (1991) 271.

[19] N. S. Amelin, H. Stöcker, W. Greiner, N. Armesto, M. A. Braun and C. Pajares, Santiago preprint US–FT/1–94 (1994) (submitted to Phys. Rev. **C**).

[20] J. Schwinger, Phys. Rev. **82** (1951) 664.

[21] A. Casher, H. Neunberg and S. Nussinov, Phys. Rev. **D20** (1979) 179.

[22] M. Gyulassy and A. Iwazaki, Phys. Lett. **B165** (1985) 157.

[23] A. Capella, C. Pajares and A. V. Ramallo, Nucl. Phys. **B241** (1984) 75; C. Pajares, Nucl. Phys. **A418** (1984) 613.

[24] K. Braune *et al.*, Phys. Lett. **B123** (1983) 467.

[25] M. A. Faessler, Nucl. Phys. **A400** (1983) 525c.

[26] N. S. Amelin, N. Armesto, M. A. Braun, E. G. Ferreiro and C. Pajares, Santiago preprint US–FT/3–94 (1994) (submitted to Phys. Rev. Lett.).

[27] K. Werner and J. Aichelin, Phys. Lett. **B308** (1993) 372.

[28] K. Werner, Phys. Rev. Lett. **73** (1994) 1594.

[29] A. Capella and A. Krzywicki, Phys. Rev. **D18** (1978) 4120; A. Capella and J. Tran Thanh Van, Z. Phys. **C18** (1983) 85; Phys. Rev. **D29** (1984) 2512.

[30] S. Uhlig, I. Derado, R. Meinke and H. Preissner, Nucl. Phys. **B132** (1978) 15.

[31] K. Alpgård *et al.*, Phys. Lett. **B123** (1983) 361.

[32] I. Derado *et al.*, Z. Phys. **C40** (1988) 25.

Table Captions

Table 1. Monte Carlo results without ($NOFUS$) and with (FUS) string fusion for the slope b in different collisions and at different energies, compared with the existing experimental data ($Exp.$) ([30, 31, 32]). The number of generated events is given, together with the definitions of the backward (B) and forward (F) regions.

Figure Captions

Figure 1. KNO plot for $PbPb$ collisions at $p_{lab} = 200\ GeV/c$ per nucleon. Black points: results from the Monte Carlo code without fusion; crosses: results with fusion.

Figure 2. The same as Fig. 1 for SS collisions at $\sqrt{s_{NN}} = 200\ GeV$.

Figure 3. The same as Fig. 1 for $CuCu$ collisions at $\sqrt{s_{NN}} = 200\ GeV$.

Figure 4. Distribution in the number of charged particles for $CuCu$ collisions at $\sqrt{s_{NN}} = 200\ GeV$. Black points: results from the Monte Carlo code without fusion; crosses: results with fusion.

Figure 5. Comparison between Monte Carlo results (with fusion: open circles; without fusion: crosses) and experimental results (black points with errors bars, [24]) for $(Dp_\perp / < p_\perp >)^2$ vs. the inverse number of charged particles for pp collisions at $\sqrt{s} = 63\ GeV$.

Figure 6. The same as Fig. 5 for $p\alpha$ collisions at $\sqrt{s} = 44\ GeV$.

Figure 7. The same as Fig. 5 for $\alpha\alpha$ collisions at $\sqrt{s} = 31.2\ GeV$.

Figure 8. Monte Carlo results (with fusion: open circles; without fusion: crosses) for $(Dp_\perp / < p_\perp >)^2$ vs. the inverse number of charged particles for SPb collisions at $\sqrt{s_{NN}} = 200\ GeV$.

Figure 9. Monte Carlo results (with fusion: open symbols; without fusion: black symbols) for $\rho_{n_{ch}}(0)/\rho(0)$ vs. $z = n_{ch} / < n_{ch} >$ for $PbPb$ collisions at $\sqrt{s_{NN}} = 6300\ GeV$.

Figure 10. The same as Fig. 9 for $CuCu$ collisions at $\sqrt{s_{NN}} = 200\ GeV$.

Figure 11. Monte Carlo results (with fusion: black points; without fusion: crosses) for D^2_{BF} taking events with a number of charged particles greater than $n_{ch,thres}$ for $PbPb$ collisions at $p_{lab} = 200\ GeV/c$ per nucleon.

Figure 12. The same as Fig. 11 for $CuCu$ collisions at $\sqrt{s_{NN}} = 200\ GeV$.

Table 1

Reaction	Regions		b	
	$B \equiv$	$F \equiv$		
pp at 45 GeV, 10000 events	$\eta < -1$	$\eta > 1$	$NOFUS$	0.13
			FUS	0.11
			$Exp.$	0.137 ± 0.023
$\bar{p}p$ at 540 GeV, 50000 events	$\eta < -1$	$\eta > 1$	$NOFUS$	0.55
			FUS	0.53
	$-4 \leq \eta \leq -1$	$1 \leq \eta \leq 4$	$Exp.$	0.41 ± 0.01
pp at 19.4 GeV, 10000 events	$0.75 < y_{lab} < 1.75$	$3.25 < y_{lab} < 4.25$	$NOFUS$	0.04
			FUS	0.04
			$Exp.$	-0.01 ± 0.01
pAr at 19.4 $AGeV$, 10000 events	$0.75 < y_{lab} < 1.75$	$3.25 < y_{lab} < 4.25$	$NOFUS$	0.33
			FUS	0.33
			$Exp.$	0.28 ± 0.04
pXe at 19.4 $AGeV$, 10000 events	$0.75 < y_{lab} < 1.75$	$3.25 < y_{lab} < 4.25$	$NOFUS$	0.37
			FUS	0.35
			$Exp.$	0.41 ± 0.04

Fig. 1

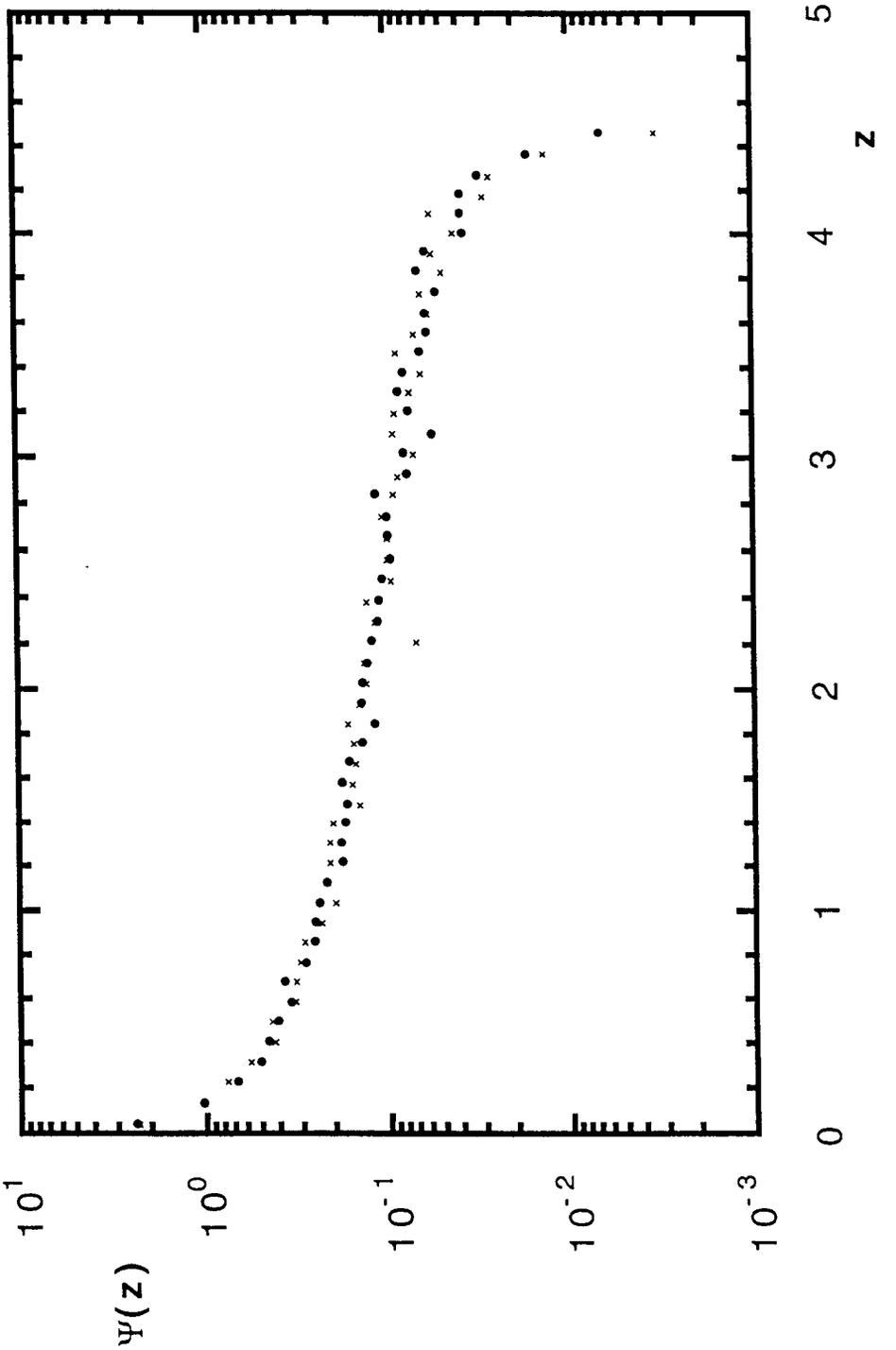

Fig. 2

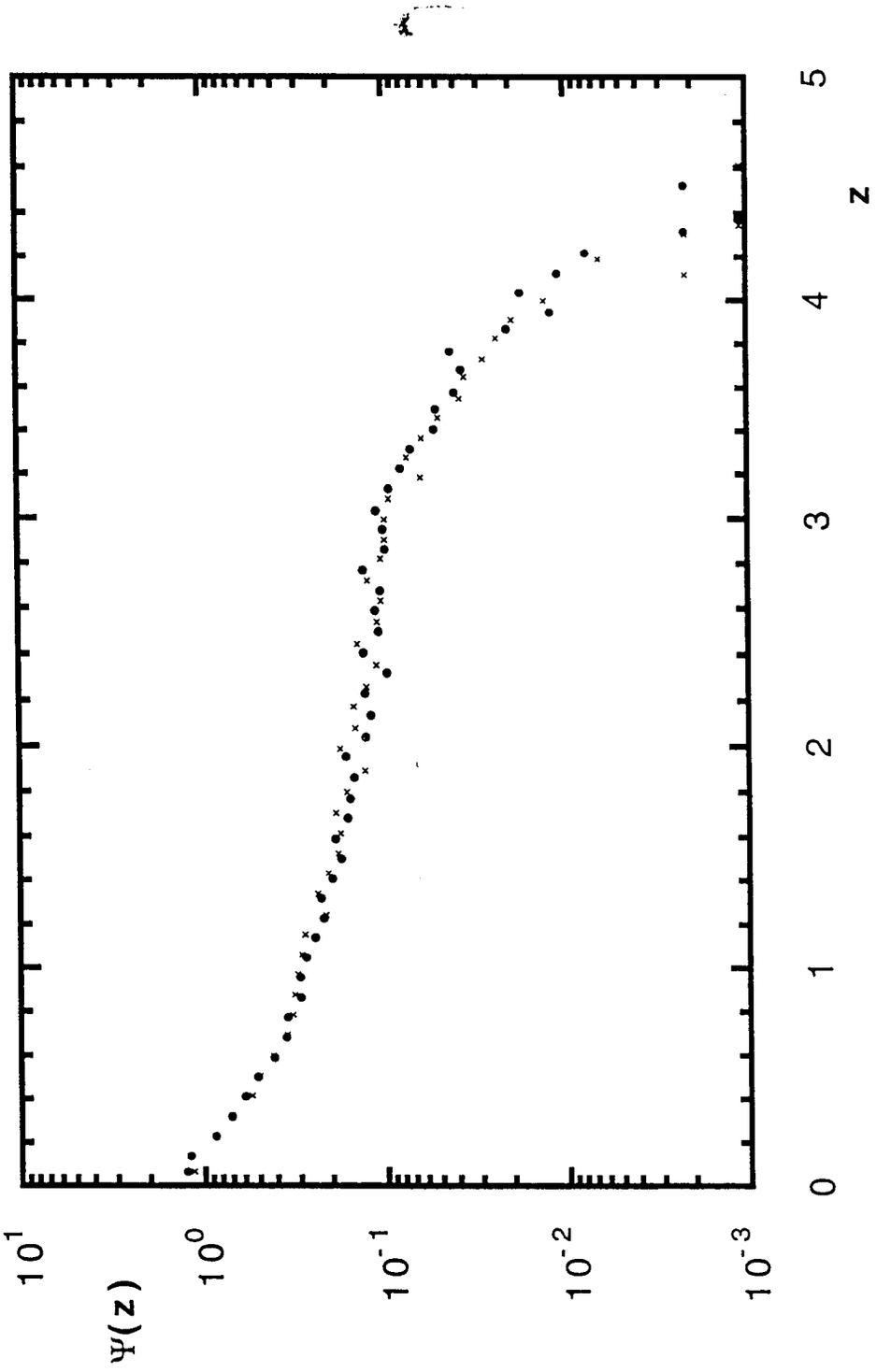

Fig. 3

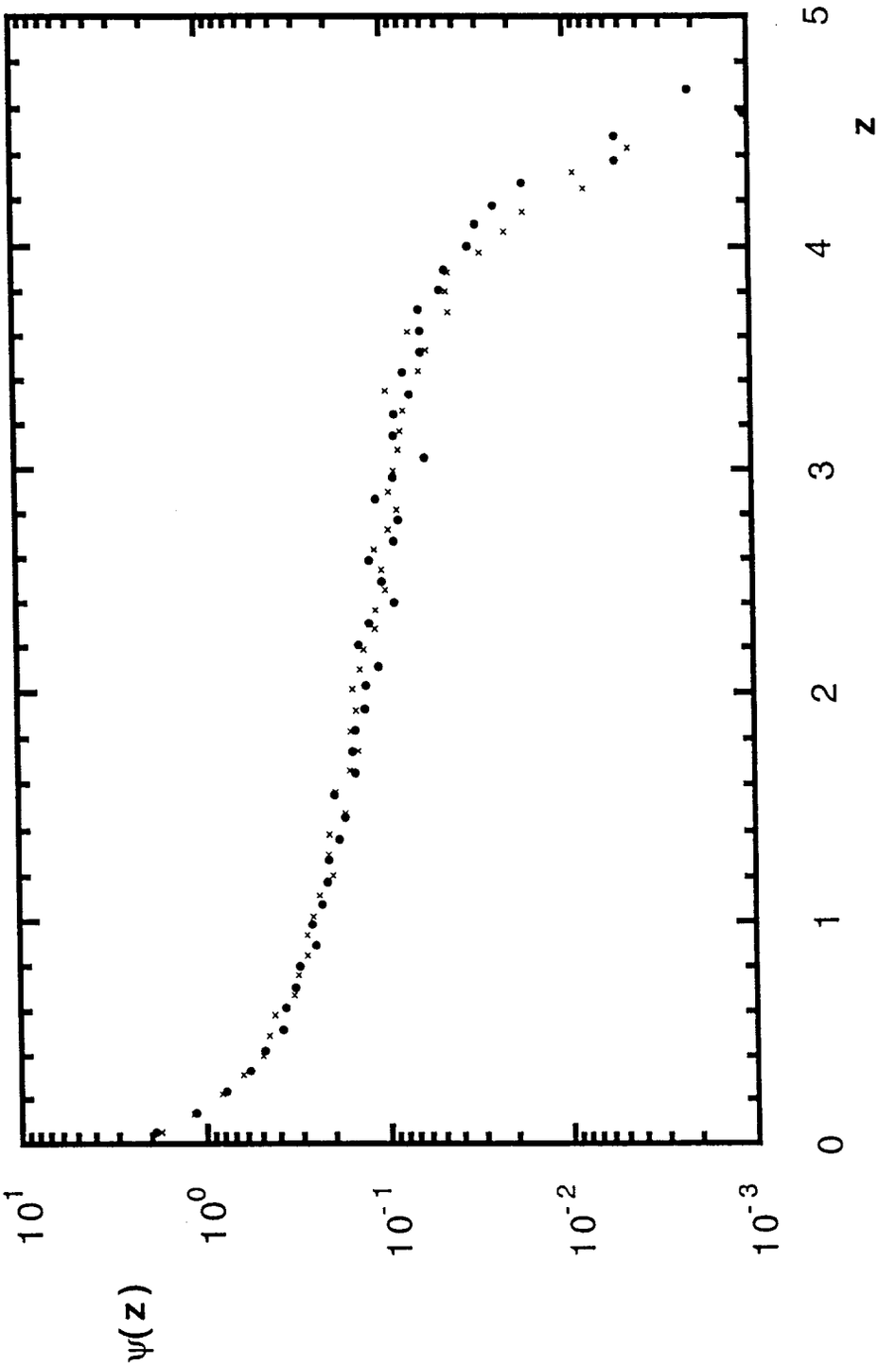

Fig. 4

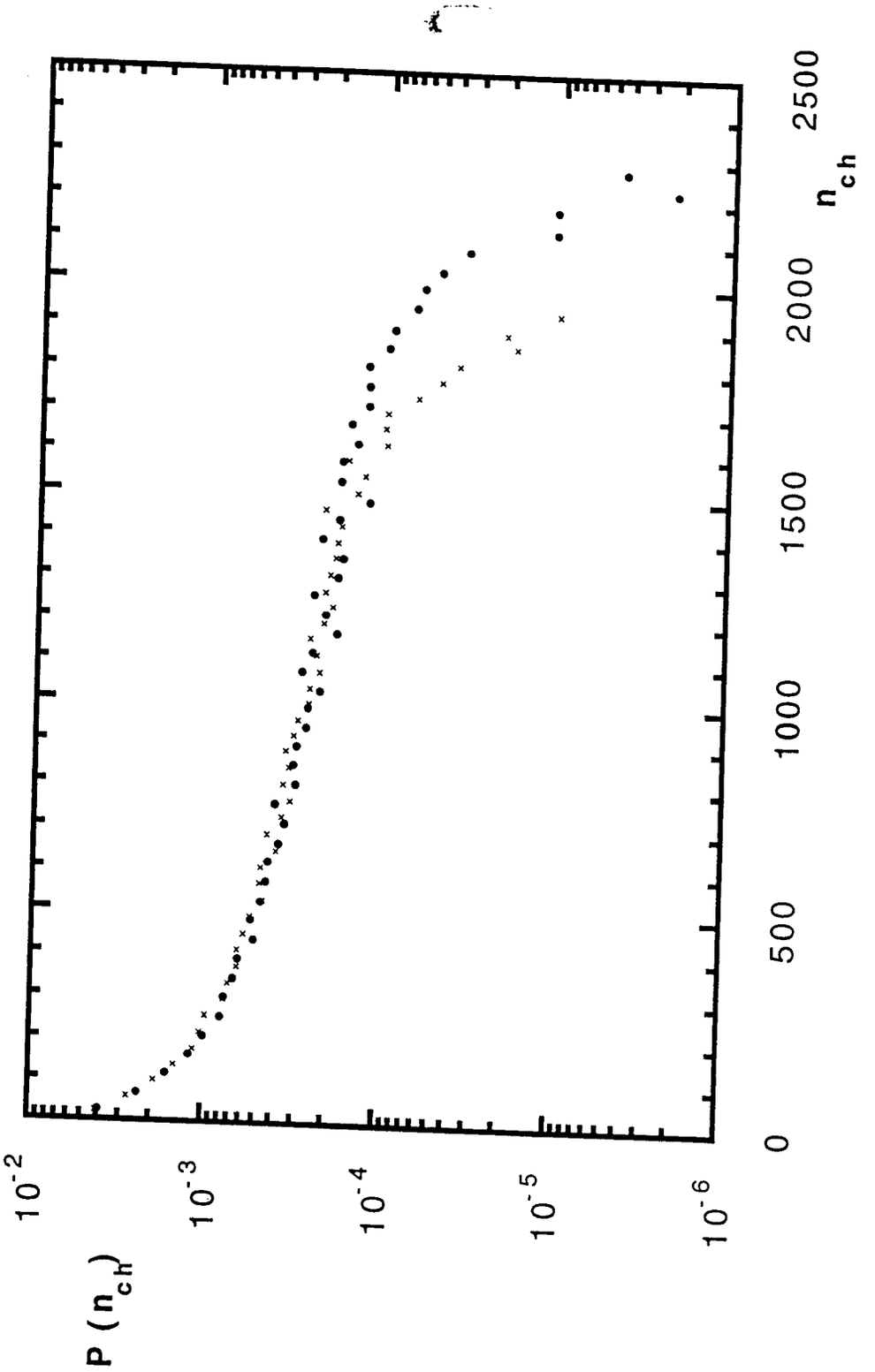

Fig. 5

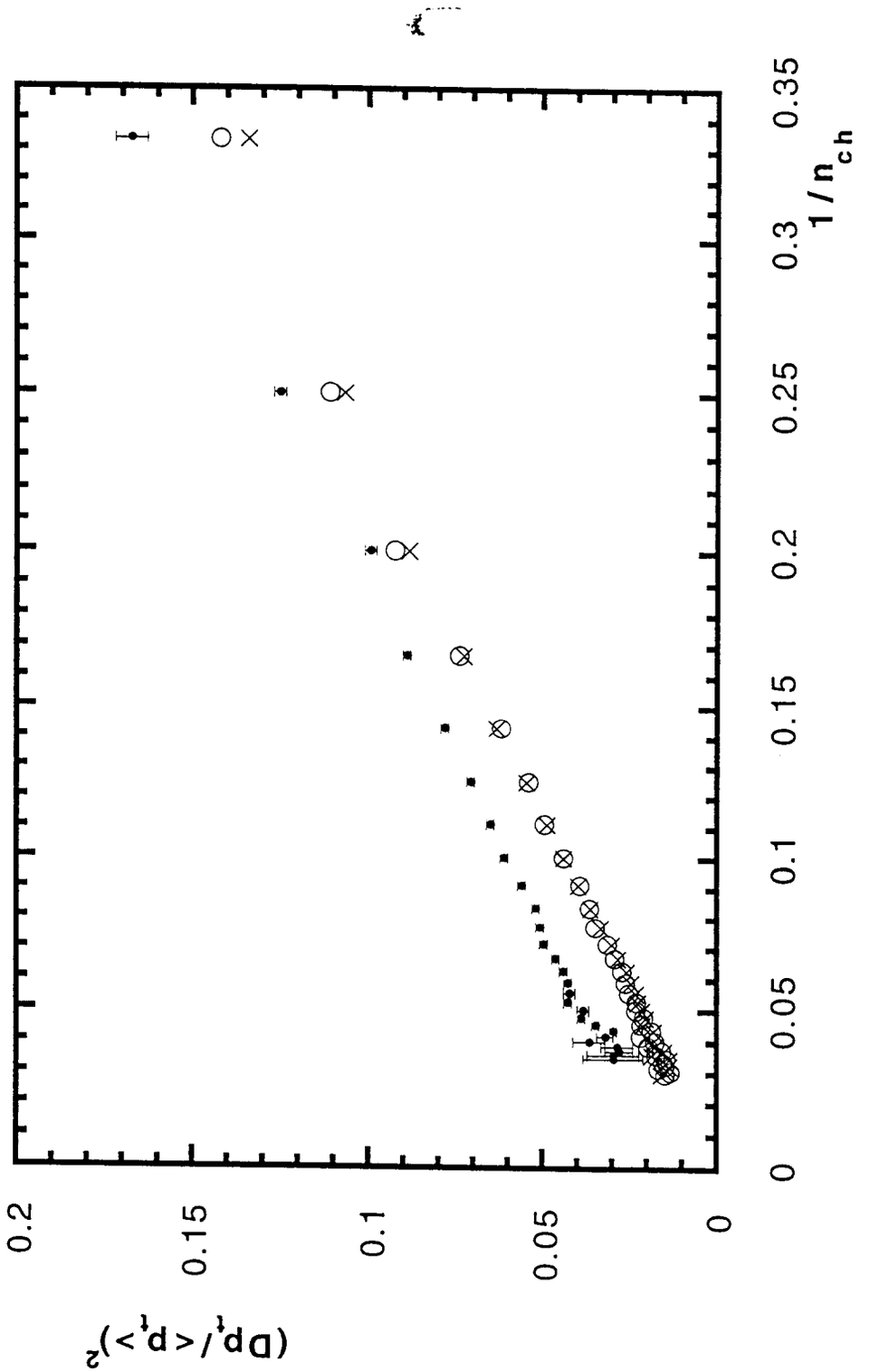

Fig. 6

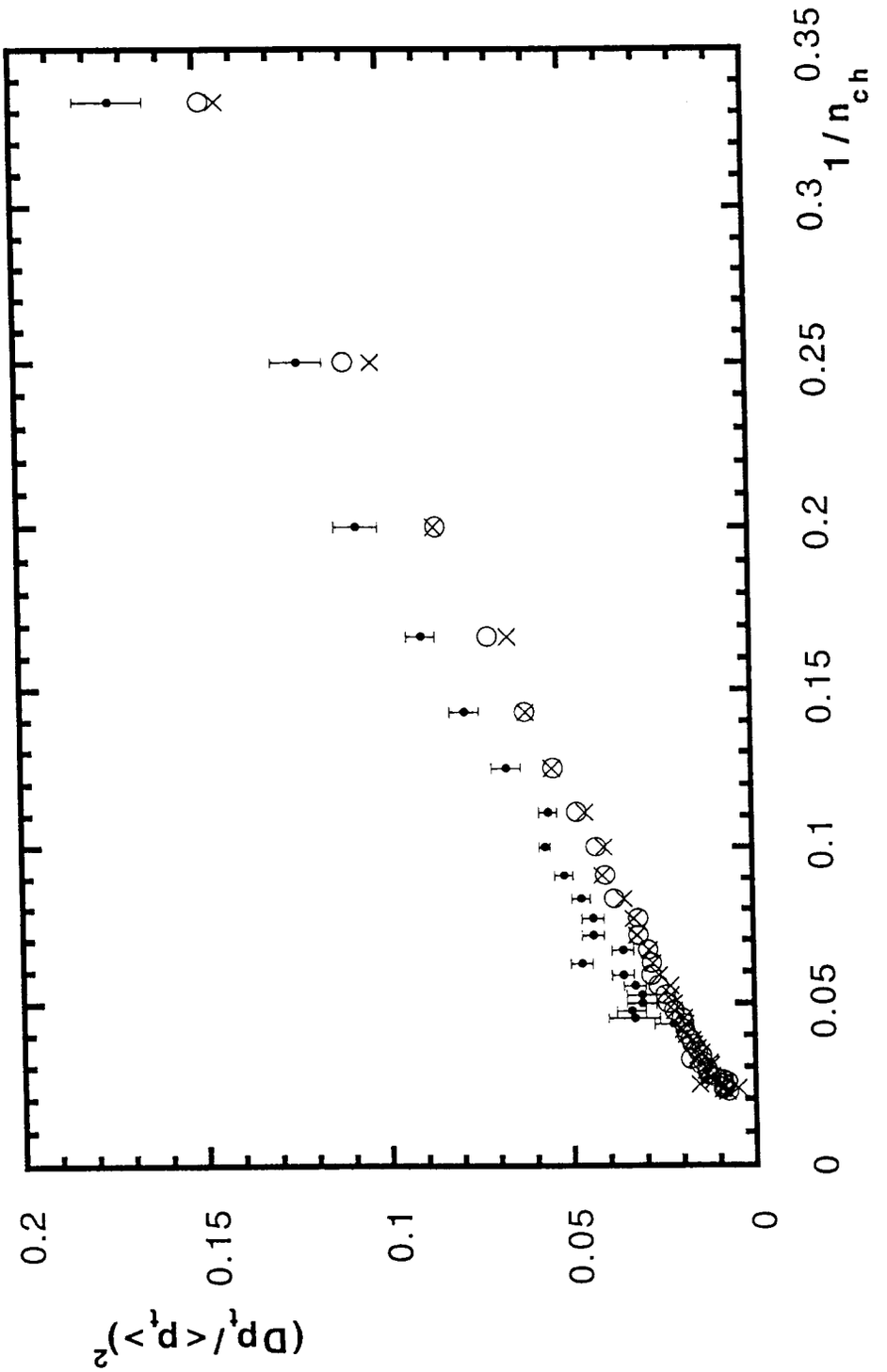

Fig. 7

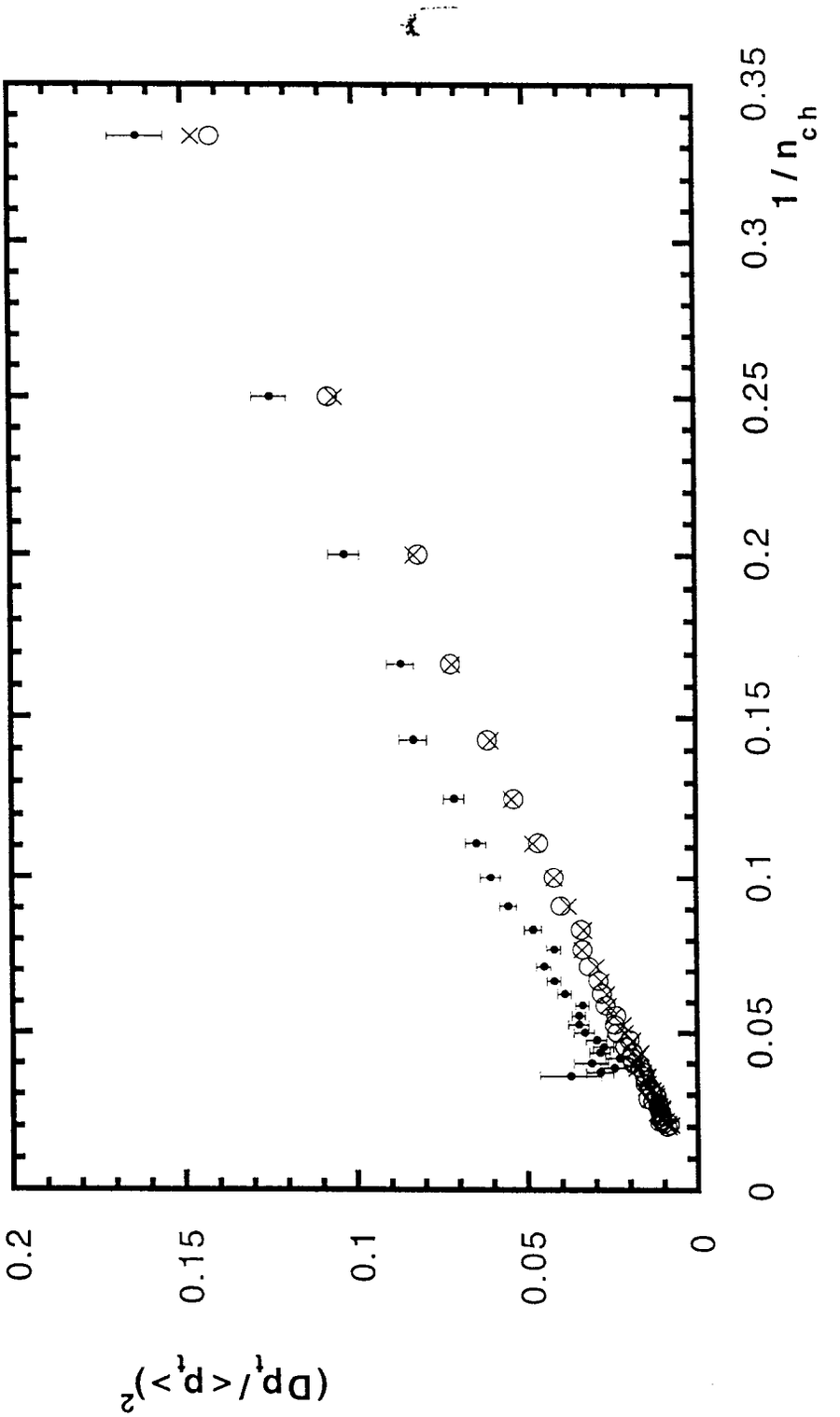

Fig. 8

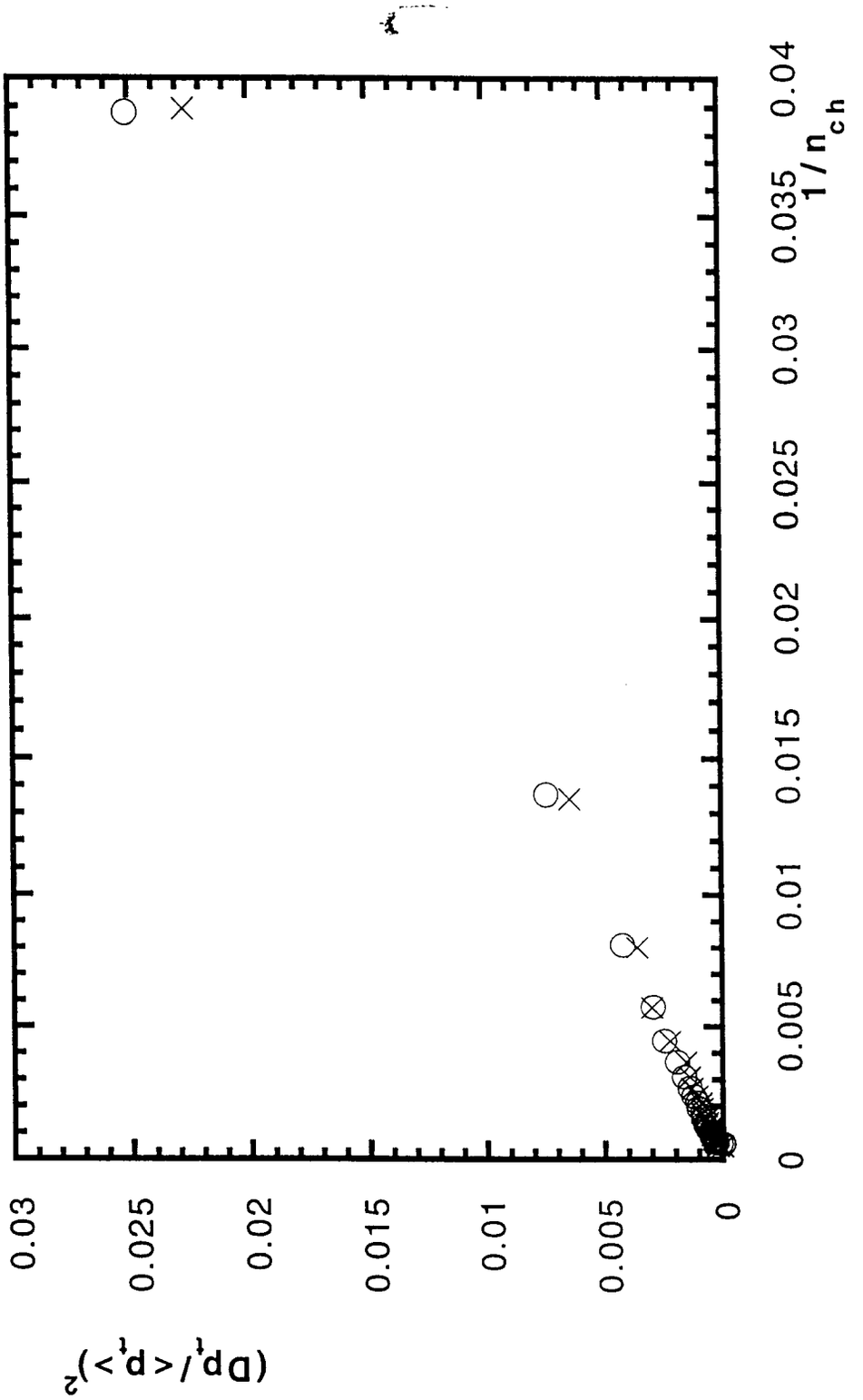
0.03
0.025
0.02
0.015
0.01
0.005
0
$(Dp_t/<p_t>)^2$
0
0.005
0.01
0.015
0.02
0.025
0.03
0.035
0.04
$1/n_{ch}$

Fig. 9

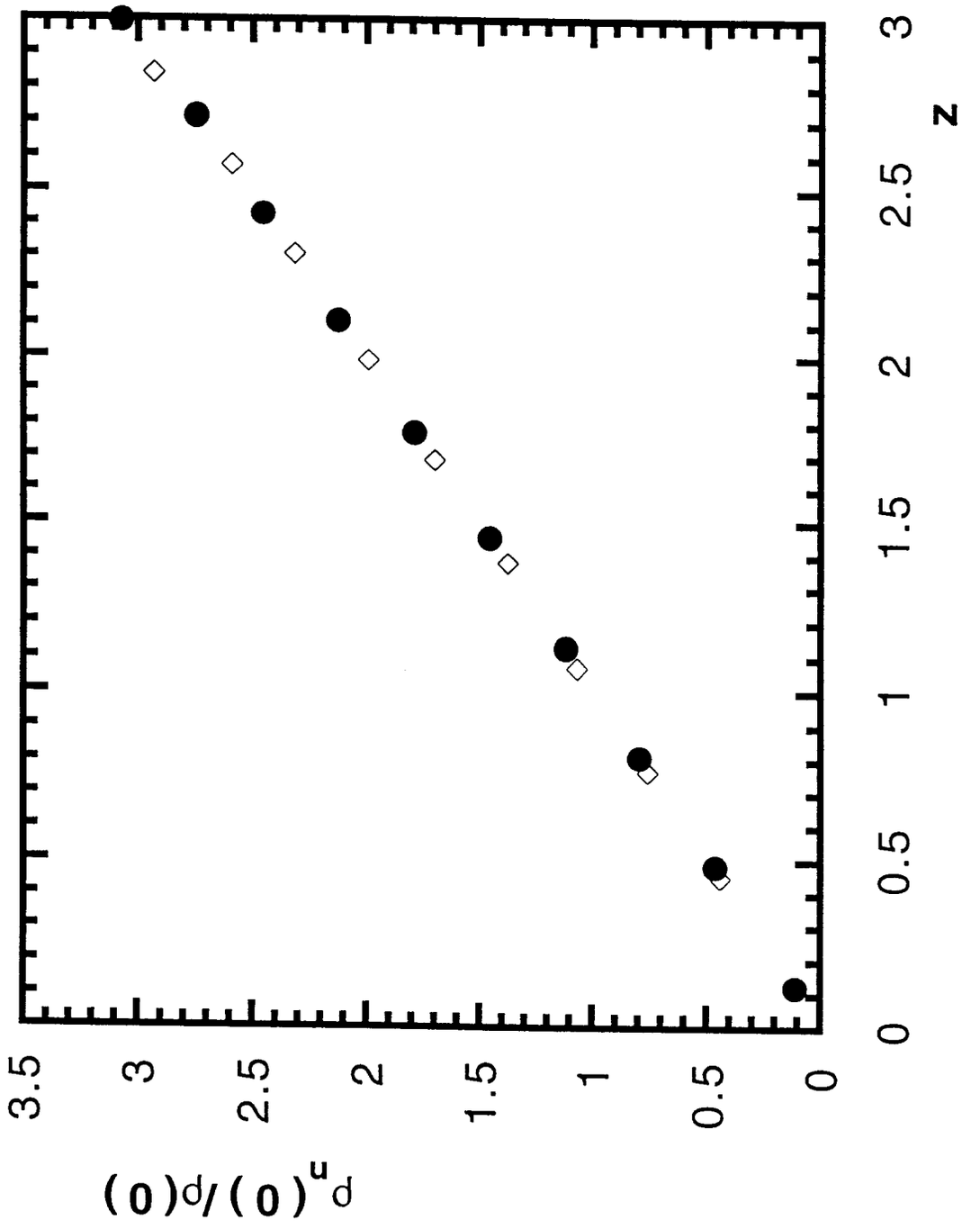

Fig. 10

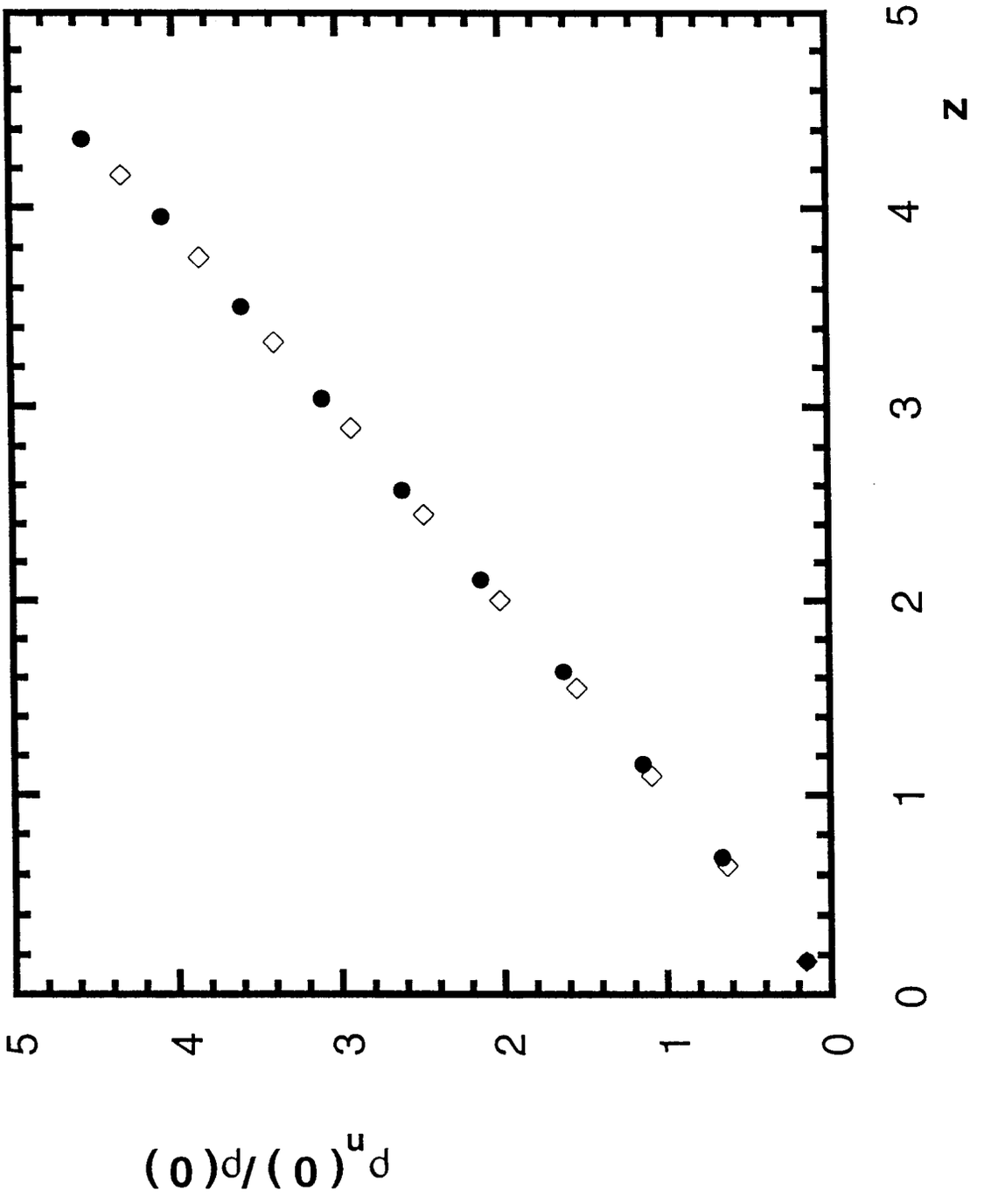

Fig. 11

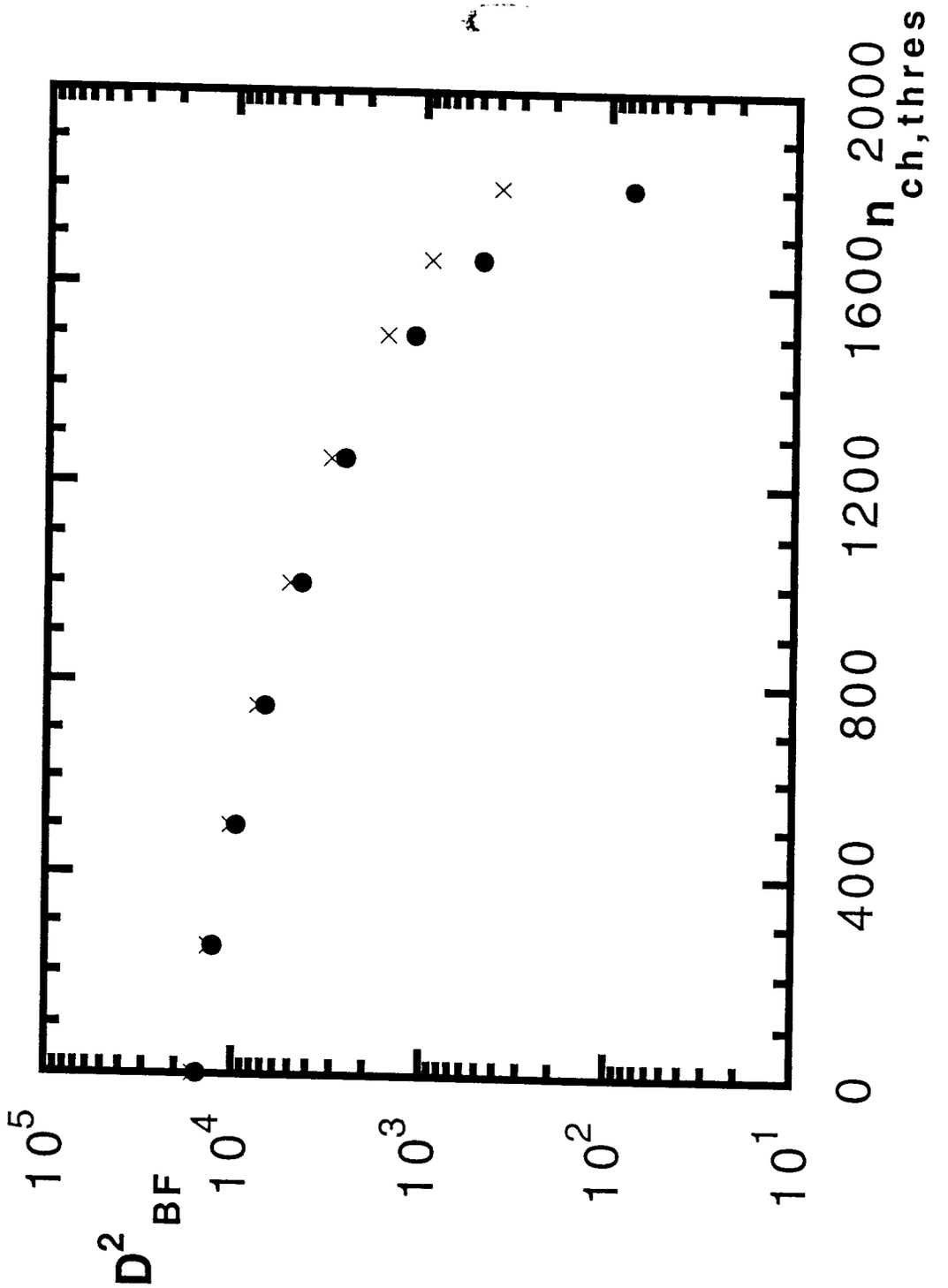

Fig. 12